# Enhancing brightness of Lambertian light sources with luminescent concentrators: the light extraction issue

T. Gallinelli, A. Barbet, F. Druon, François Balembois, Patrick Georges, T. Billeton, S. Chénais, S. Forget

Research Article | Vol. 27, No. 8 | 15 Apr 2019 | OPTICS EXPRESS 11830
Optics EXPRESS

# Enhancing brightness of Lambertian light sources with luminescent concentrators: the light extraction issue

T. GALLINELLI,[1] A. BARBET,[2] F. DRUON,[2] F. BALEMBOIS,[2] P. GEORGES,[2] T. BILLETON,[1] S. CHENAIS,[1,*] AND S. FORGET[1]

[1]*Laboratoire de Physique des Lasers, UMR 7538 CNRS, Université Paris 13, Institut Galilée, 99 avenue Jean-Baptiste Clément, 93430 Villetaneuse, France*
[2]*Laboratoire Charles Fabry, Institut d'Optique Graduate School, CNRS, Université Paris-Saclay, 91127 Palaiseau Cedex, France*
**sebastien.chenais@univ-paris13.fr*

**Abstract:** Luminescent concentrators (LC) enable breaking the limit of geometrical concentration imposed by the brightness theorem. They enable increasing the brightness of Lambertian light sources such as (organic) light-emitting diodes. However, for illumination applications, light emitted in the high-index material needs to be outcoupled to free space, raising important light extraction issues. Supported by an intuitive graphical representation, we propose a simple design for light extraction: a wedged output side facet, breaking the symmetry of the traditional rectangular slab design. Angular emission patterns as well as ray-tracing simulations are reported on Ce:YAG single crystal concentrators cut with different wedge angles, and are compared with devices having flat or roughened exit facets. The wedge output provides a simple and versatile way to simultaneously enhance the extracted power (up to a factor of 2) and the light directivity (radiant intensity increased by up to 2.2.)



## 1. Introduction

Light-emitting diodes (LEDs) are not only the new reference for general lighting, they have also proved to be reliable and economically-viable alternatives to halogen or arc lamps for more specific, bright illumination sources useful for *e.g.* automotive [1] or medical applications [2]. LEDs have also recently shown their potential as lower-cost alternatives to lasers or laser diodes for laser pumping [3–5]. More recently, Organic Light-emitting diodes have also emerged as flat, potentially flexible, large-area lighting devices with high potential in lighting, optical communications [6] or medical care [7]. Many of those novel applications triggered by the availability of these sources require the beam to be not only intense but also directional, which enables for example the light beam to be tightly focused. This is challenging with LED chips or OLED panels as their emission is not directional but quasi-Lambertian: their radiance — also referred to as "brightness", that is power per unit apparent area and solid angle — is independent of observation angle. The brightness theorem [8] indeed states that the irradiance (in $W/m^2$) produced at some remote location by a Lambertian source, will be always lower than the irradiance measured directly onto the exit surface of the emitter (*i.e.*, the source power density). This is important pointing out that this result remains true whatever the nature (imaging or non-imaging) of the optical system between the source and detector, and no matter the number of individual emitters that one could possibly imagine to combine alongside. However, if light is not just refracted or reflected but instead absorbed and reemitted at a lower energy, through a luminescence process, overcoming the brightness theorem becomes possible: this is the key idea behind Luminescent Concentrators (LC). LCs have been proposed in 1976 in the context of photovoltaics to concentrate sunlight with a wide field of view and no need for tracking [9–11]. They consist in a slab of a solid-state fluorescent material surrounded by air (or more generally a lower index material) in which

#357320 https://doi.org/10.1364/OE.27.011830
Journal © 2019 Received 10 Jan 2019; revised 21 Feb 2019; accepted 26 Feb 2019; published 12 Apr 2019

Optics EXPRESS

luminescence is guided by Total Internal Reflection (TIR) towards the edges, where the irradiance can reach values higher than the irradiance of incoming radiation by typically one order of magnitude in most practical cases. More recently, LCs have been used in association with LEDs disposed on the top largest surface to produce irradiances that could not be accessible with LEDs alone: this for instance enabled Ti-Sapphire lasers to be pumped for the first time by LEDs [12]. This example shows that the association of planar Lambertian LED light sources with LCs opens a novel route for high-brightness illumination sources that furthermore extends the wavelength capabilities of available LEDs. However, using LED + LC combinations to build bright directional sources requires that the radiation emitted in a high-index material is eventually outcoupled to air, which raises the important issue of light extraction, a long-studied issue in other contexts like device design of LEDs [13], OLEDs [14] or scintillators [15].

In planar light-emitting devices, classical strategies for light extraction include *e.g.* surface texturing [16], or surface modification with microlens arrays [17], networks of inverted micropyramids [18] or photonic crystal nanostructures [19]. For LCs based on plastic or crystalline slabs, the realization of such micro or nanostructures is both complicated and costly. The idea to change the geometry of the LC on the macroscopic scale has been investigated by De Boer et al. [20] who proposed to use a Compound Parabolic Concentrator (CPC) attached to the edge: the CPC both increases the emitting area and decreases the emission solid angle (as the *étendue* is conserved in a passive optical device) but it offers a way out for trapped rays (defined in following section): in the end, the outgoing radiation has a reported brightness that is 4.5 times higher than the brightness of LED illumination, and is more directional.

In this paper we study how more cost-effective and universal techniques can be used to improve the extraction capabilities and beam characteristics of concentrators that are used in the context of illumination. Firstly (section 2), we present a simple graphical representation in k space that enables an easy classification of rays inside a concentrator, offering a convenient tool for making rapid estimates but also understanding what happens in situations where the concentrator loses some of its symmetries. We then present the experimental methods and compare the measurements of concentration factors of a simple rectangular polished slab concentrator with a concentrator in which the output facet is simply frosted (section 3). In section 4, we investigate an original and simple way to improve light extraction from luminescent concentrators, applicable to any material, consisting in cutting the exit facet with a wedge. We studied Ce:YAG single crystals, chosen for their attested very good efficiency as luminescent concentrators under blue LED excitation [21]. The impact of the design on the achievable gain in extracted power, intensity and radiance (brightness) will be finally discussed.

## 2. Light extraction in luminescent concentrators: representation of internal rays in *k* space

It is first instructive to gain some insights in the light extraction issue in the "classical" symmetric rectangular slab design, considered polished on its 6 orthogonal faces, to investigate how this design can be further modified to improve extraction. In this respect, an elegant and insightful picture consists in representing rays only by their direction (in *k* space). Usually the problem of extraction is considered in planar light sources (LEDs, OLEDs…), where one dimension is much smaller than the others: in this case, all internal rays that fall within the escape cones (and only 2 cones are considered, with axes normal to the source plane) are directly outcoupled without undergoing any total internal reflection before exiting, while all the others are referred to as "guided rays", and are subsequently either absorbed, scattered, or coupled to other surface modes. In a 3D macroscopic geometry all 6 faces can contribute to TIR, and escape cones have to be considered on every face of the concentrator.

Optics EXPRESS

Escape cones in a rectangular slab of index $n$ of any dimension surrounded by air appear as cones of solid angle $\Omega_{escape} = 2\pi(1-\cos\theta_{crit})$ where $\theta_{crit}$ is the critical angle (see Fig. 1).

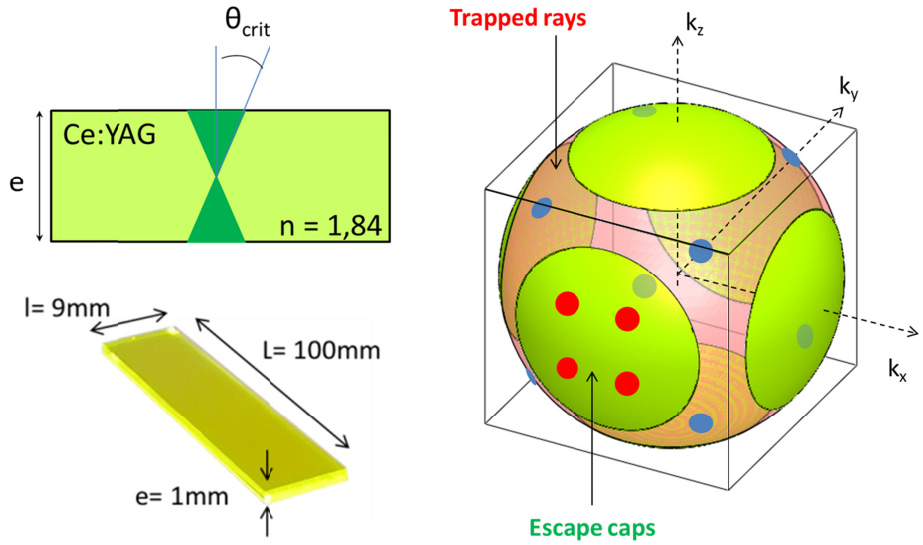


**Fig. 1.** Left: geometry of the of the Ce:YAG slab concentrator. Right: representation in k space of internal rays in a reabsorption-free concentrator. The blue circle dots picture a possible trajectory of a "trapped ray" which cannot escape throughout any of the 6 faces. Red dots in the escape cap represent the 4 possible k vectors that a ray exiting by the front smallest facet can take: its $k_y$ component is conserved while the other components bounce between $\pm k_x$ and $\pm k_z$, still remaining inside the same "escape cap" (see text for more details).

These cones can be considered as being inside a sphere of radius $n = k/k_0$ (modulus of k vector inside the medium normalized to its value in the surrounding medium). Escape cones intersect the sphere under the form of 6 symmetric "caps", which can be also seen as the outermost part of the sphere emerging out of an 'extraction cube' whose edges equal $2\sqrt{n^2-1}$ (Fig. 1, right).

As far as the caps do not overlap, knowing the direction of a ray is enough to unambiguously tell from which of the 6 facets this ray will emerge (if it does), *whatever the number of TIR the ray may undergo afterwards and the position of the source*. Note that caps do not overlap whenever the critical angle is below 45° (the situation where the six caps are tangent), that is for $n$ higher than $\sqrt{2}$ : this condition is actually met in all practical plastics, glasses or crystalline materials that can be used as concentrators. Considering isotropic emitters with no reabsorption and neglecting Fresnel reflections below the critical angle, the fraction of light that can escape to air from an isotropic medium of index $n$ is simply given by

$$\eta_{escape} = \frac{\Omega_{escape}}{4\pi} = \frac{1}{2}\left[1-\sqrt{1-\frac{1}{n^2}}\right] \qquad (1)$$

and is only 8% for YAG (n = 1.84). This fraction is theoretically independent on the facet dimensions, meaning that the same luminous power flows through all 6 faces, a result that is not that intuitive and in fact very difficult to observe experimentally due to the large influence of self-absorption effects in the physics of luminescent concentrators [22].

The sphere in $k$ space enables a very graphical and useful representation of 'trapped rays'. The trapped rays are defined as rays undergoing Total Internal Reflection *on all 6 faces*. Those rays can find endless closed loop trajectories in a lossless medium: they exist whenever

Optics EXPRESS

the sphere is not totally paved by escape caps, that is when the diagonal of the extraction cube is longer than the sphere diameter — that is, for $n > \sqrt{3/2} = 1.22$

For non-overlapping caps ( $n > \sqrt{2} = 1.41$ ), they represent a fraction

$$\eta_{trapped} = 1 - \frac{6\Omega_{escape}}{4\pi} = 3\sqrt{1 - \frac{1}{n^2}} - 2 \quad (2)$$

for YAG, $\eta_{trapped} = 52\%$.

Each Total Internal Reflection (TIR) changes sign of $k_x$, $k_y$ or $k_z$: the trajectory of a "trapped ray" in k-space is therefore figured by the 8 apices (blue dots in Fig. 1) of a parallelepiped inscribed in the sphere. When considering a ray that belongs to an escape cone (let's say the cone with $k_y<0$, see red dots in Fig. 1), the $k_x$ and $k_z$ components can change sign many times when the ray is travelling but $k_y$ is conserved. The trajectory is then represented in k-space by a dot bouncing between 4 points with the same $k_y$ component, always remaining within the same escape cap, before the ray can eventually exit — the number of reflections undergone by a ray will obviously depend on the position of the luminophore with respect to the exit surface.

In practice, scattering and reabsorption complicates this simple sketch: rays that experience propagation paths that are longer than the reabsorption length will not necessarily escape by the facet defined by the initial ray direction. Trapped rays will acquire a finite lifetime and will not bounce "forever". In high-quality crystals with large Stokes shift, the reabsorption length can however be quite high. In the Ce:YAG samples used in our study (see next section), the reabsorption length, which is simply estimated here from the inverse of the average absorption coefficient weighted by the fluorescence spectrum, is 3.4 cm, while the typical slab dimensions are in the mm to cm range. As a general rule of thumb, this framework for representing concentrators is useful in cases where the reabsorption length is longer than the typical dimensions of the concentrators.

The concept is here introduced in the simplest case of a symmetric (3 pairs of mutually parallel facets) optically-isotropic medium surrounded by a homogeneous isotropic medium. It can be especially useful however in more complex situations: for instance, the sphere becomes ellipsoids in anisotropic media; the caps may also have different dimensions if the surrounding medium is not homogeneous, which is the case if the concentrator slab sits on top of a substrate, for example.

In these non-trivial cases, the "trapped ray" area is determined by mapping the zones that are not covered by any cap *and* by any cap mirror-image: indeed, one has also to remove from the trapped ray region all the rays that will find themselves into an escape cap after one or several reflections. This means that one has to pave the sphere with all the mirror images of the caps through all the symmetry planes (where TIR can occur) to determine what is finally the 'trapped ray' (uncovered) region.

From this example, one can see that breaking the symmetry is a simple and efficient strategy to eliminate the existence of trapped rays, and hence improve the fraction of rays that can potentially be outcoupled.

In this paper, we investigated how a simple wedge in one direction, appended to the small exit facet, can significantly improve light extraction.

In this graphical representation in *k* space, tilting the output facet by an angle β consists in sliding the escape "cap" of the side edge towards the "pole" (top face escape cone), as represented in Fig. 2. Not only will the rays belonging to this tilted escape cap emerge, but also all those which find themselves in this cap after TIR. As the faces perpendicular to $k_z$ are the largest — so that most of TIR events occur on those facets — the new escape cone has to be completed by its mirror image across z axis: tilting the facet therefore increases notably the surface of the sphere that is paved by escape cones. Note that the tilted facet is also still a

Optics EXPRESS

possible surface for TIR, especially here for rays with a small $k_z$ component that will not emerge any more through the flat side facet but instead from the bottom side, near the apex. These rays would be visualized by representing the symmetric of the bottom cap with respect to the plane of the tilted facet. New overlaps appear, representing directions of rays for which several exit facets are possible.

In the end, the loss of symmetry covers the sphere almost continuously by successive images of the tilted cap and hinders trapped ray trajectories to exist anymore, except here within a thin stripe on the edges (see Fig. 2) Note that complete removal of trapped rays would be straightforwardly obtained by tilting the wedge with an oblique angle.

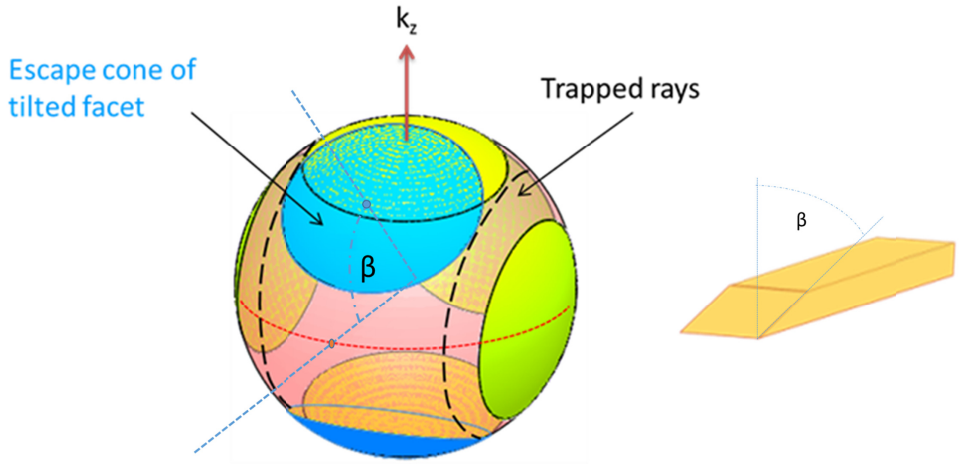


**Fig. 2.** A wedged concentrator (on the right) in k space (on the left, partial representation). Rays that can escape through the tilted up facet belong to the tilted escape cone slided upwards on the sphere by same polar angle β (on top side, hatched), but may also belong to its mirror image about z axis (bottom side, hatched). To determine whether some "trapped" rays still exist, escape caps and all their images about all possible mirror symmetries have to be drawn: here, a thin stripe of trapped rays remains for some oblique rays. Note: rays exiting the bottom extremity are given by the image of bottom cap about the plane tilted by angle β (not shown).

## 3. Experimental methods: comparison of light extraction between polished and unpolished exit facets in symmetric rectangular slab concentrators

We first measured experimentally the concentration factor of a Ce:YAG single crystal rectangular slab (St Gobain) of 49 × 9 × 1 mm (L × l × e) dimensions, polished on its 6 faces, hereafter referred to as the "reference" sample. The largest area of the rectangular slab was uniformly illuminated by a low-coherence (speckle-free) 450-nm laser diode whose beam was homogenized to yield a constant power density of 0.48 mW/cm$^2$. The $Ce^{3+}$ doping ratio was around 0.3 at.% (supplier estimate) resulting in an experimental 97.5% ± 0.5% absorption along 1 mm at 450 nm. The extracted luminescence power was measured using an integrating sphere (GL Optisphere 205). To ensure that the sphere efficiently collects all the light emitted by the edge, the LC was pushed inwards inside the sphere throughout a rectangular fitted aperture, thus reducing the effective illumination area to 42 × 9 mm$^2$. In the following, all concentrators have a geometrical concentration factor G = L/e = 42 (see notations in Fig. 1)

In the reference sample, the ratio of output power $P_{ref}$ over the incident pump power $P_{inc}$ was measured to be $\eta = 12\%$ leading to a concentration factor $C = G \times \eta = 5.04$.

In order to compare this value with theoretical estimates based on "ratio of rays" that exit through the exit surface (or equivalently in terms ratio of photons), this power ratio has to be converted in a ratio of outcoupled photons over a number of incident photons and reaches 14.1% given the Stokes shift between absorption and fluorescence mean wavelength. In the

Optics EXPRESS

previous section, we estimated the fraction of photons outcoupled by the side facet to be 8% of the total number of photons generated inside a perfect lossless concentrator. As all incident photons are not absorbed and as all absorbed photons are not reemitted as fluorescence (*i.e.* pump absorption efficiency and fluorescence Quantum yield are below unity), we can expect a theoretical ratio of outcoupled photons over incident photons slightly lower than 8%: in fact, the quantum yield is as high as 97% in Ce:YAG and absorption is 97.5%, which does not make so much difference. However, the experimental value is almost twice higher than the expectation from these simple considerations. This can be attributed for some part to reabsorption, which reduces the number of trapped rays and redirects them in all extraction cones. It is also due for another part to scattering on defects on the surfaces and to diffraction around sharp corners and edges. It is possible to evaluate the relative importance of reabsorption and diffraction/scattering effects, by resorting to ray-tracing simulations, which can include the effect of reabsorption but do not go beyond ray propagation considered within the limits of geometrical optics. We used Light Tools software to model a perfectly polished LC with a refractive index n = 1.84, having passive losses corresponding to a measured 97% transmission over 100 mm of propagation in Ce:YAG. Reabsorption was taken into account by considering the medium as homogeneously doped with an isotropic emitter whose absorption and emission spectra were those experimentally measured, while the luminophore concentration was calculated from the experimental absorption at 450 nm. The simulation yields a photonic extraction efficiency of 11.3% (9.6% in power ratio), meaning that starting from the rough estimate of 8% based only on geometrical considerations, reabsorption accounts for an additional 3.3%. The remaining difference of 2.8% between the experimental 14.1% efficiency and the simulated value of 11.3% is accounted by all phenomena that are not taken into account by ray tracing simulations, *i.e*. scattering and diffraction. Adding some further scattering seems to be a straightforward and simple idea to increase the light extraction, an idea that we explored in order to compare it with the wedge structure presented in the next section. The symmetric polished slab of 49 × 9 × 1 mm dimensions was left polished on 5 sides and frosted on one of the smallest facets of dimension 9 × 1 mm. The exit facet was roughened using abrasive grinding over a brass tool in order to obtain a RMS roughness of 430 nm, measured using Atomic Force Microscopy. An increase in the extracted power of up to 50% was observed, corresponding to a concentration factor of 8. The intensity indicatrix was measured in one angular dimension with a simplified version of the experiment described by Parel et al. [23] that is shown in Fig. 3a.

Optics EXPRESS

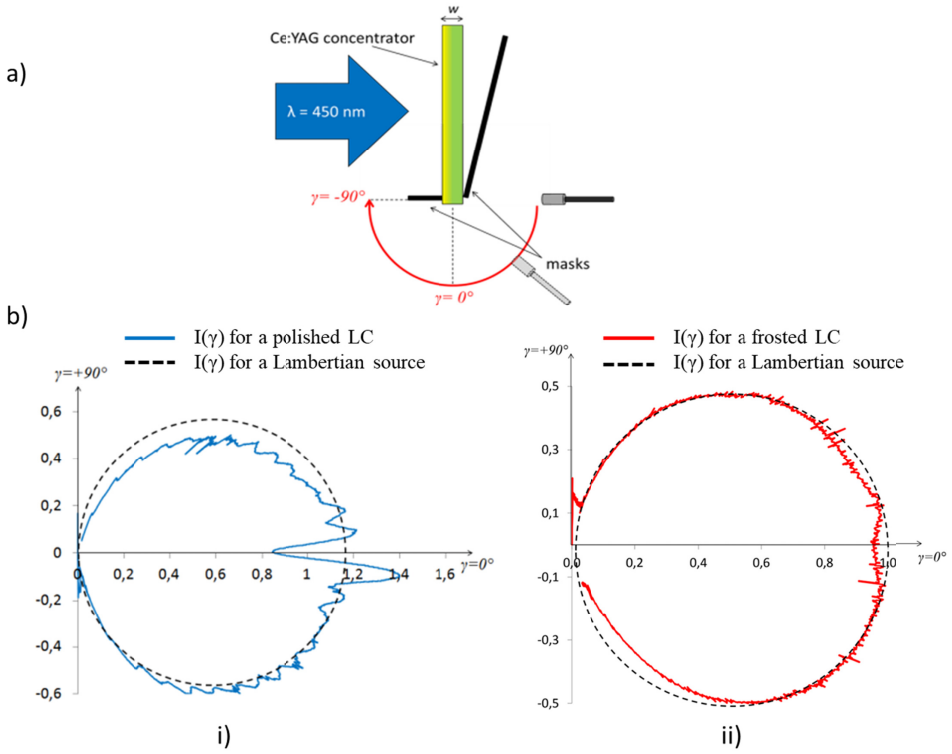


**Fig. 3.** a) experimental set up for radiant intensity indicatrix measurement. A fiber-coupled power-meter (fiber core diameter: 1 mm) rotates at a fixed distance of 70 mm around the central point of the edge emitting area of the Ce:YAG luminescent concentrator. b) Intensity profiles (the radius in the polar diagram is set proportional to the intensity in Watts per steradian in this given direction) of a Ce:YAG luminescent concentrator excited at λ = 450 nm: i) with polished emission facet ; ii) with frosted output surface. Theoretical Lambert's cosine law appears in dotted lines on i) and ii).

Intensity profiles (see Fig. 3b) reveal that both the 'polished' reference sample and the grinded one have an angle-dependent intensity that is close to Lambert's cosine law. The frosted sample is however much closer from an ideal Lambertian source than the polished concentrator, in which some smooth ripples can be observed. The origin and physical explanation of these ripples is detailed in the Appendix.

## 4. Light extraction in wedged luminescent concentrators

We then investigated the influence of a wedge on the exit facet, a way to eliminate closed ray paths that are stable upon successive TIR processes (see Fig. 2) and are responsible for the significant percentage of trapped rays propagating in a high index medium surrounded by air.

In order to experimentally investigate the role of wedging in a real device, we started from the reference Ce:YAG crystal and fabricated different samples with three wedge angles β of 20°, 40°, and 60° around a rotation axis defined as the longest edge of the exit surface (see Figs. 4 and 5).

Optics EXPRESS

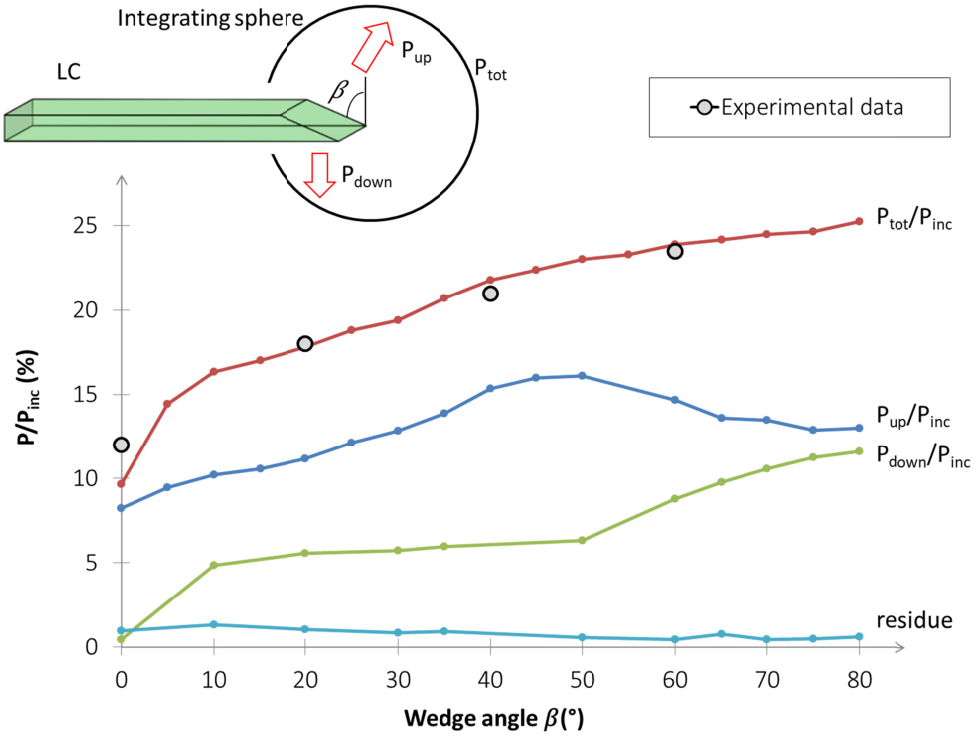


**Fig. 4.** Power extraction efficiency η measured (black dots) and simulated by ray tracing (linked crosses) for wedged concentrators with different wedge angles β. $P_{up}$ is the power extracted through the tilted output surface and $P_{down}$ is the power emitted through the bottom base of the slab inserted into the integrating sphere. $P_{residue}$ represents the remaining light emitted by the portion of small side facets inserted into the sphere. Inset: Experimental setup: the concentrator was introduced in the integrating sphere up to 1 mm behind the wedge limit on the top surface to ensure that all light coming from the wedge is efficiently collected.

The extracted measured total power $P_{tot}$ not only consists in the power emitted from the tilted surface (denoted as $P_{up}$), but also from the bottom base end ($P_{down}$), and to a lesser extent from the side facets (noted $P_{residue}$) so that $P_{tot} = P_{up} + P_{down} + P_{residue}$. Isolating the contribution from the sole wedged top side is experimentally very difficult without compromising the TIR properties of the whole device: we therefore relied on ray tracing simulations (using LightTools software) to assign the relative contribution of each emitting surface.

The measured and simulated extracted powers are reported in Fig. 4. Increasing the wedge angle results in a net higher total extracted power $P_{tot}$. Very good agreement is obtained between simulated and experimental data for $P_{tot}$ with a slight deviation for β = 0 where simulation tends to underestimate the extraction, although reabsorption is here taken into account. As discussed in section 3, this can be attributed to scattering on sharp edges and on polishing defects, especially along the lines, which reduces the fraction of trapped rays. It can also be seen that close to β = 0, the dependence with angle β is steeper: this corresponds to the fact that as far as β ≠ 0 there is mathematically no more endless closed paths corresponding to trapped rays in a perfectly lossless medium. Excellent agreement at higher angles justifies using simulation to evaluate the fractions of $P_{tot}$ that are extracted upwards, downwards, or sideways. From Fig. 4, one can clearly see an optimum angle for $P_{up}$ close to β = 50° associated to a maximum extraction efficiency $P_{up}/P_{inc}$ = 16% through the tilted surface, that is, 1.3 times more than the ratio obtained from the reference non-wedged polished slab (β =

Optics EXPRESS

0). The whole extracted power reaches 25% for large angles, twice as much as the reference. For wedge angles > 50°, rays coming from the concentrator volume will hit the top surface with an incident angle that is in average higher than the TIR limit angle $\theta_{lim}$ = Arcsin (1/n) = 33°, redirecting them to the bottom base, which explains the relative increase of $P_{down}$ at large angles.

In order to be able to characterize the brightness of the wedge LCs, we performed intensity profile angular measurements on the various wedged concentrators. The results obtained using the setup described previously (see Fig. 3 left) are shown in Fig. 5 together with simulated intensity profiles. The intensity is strongly angle-dependent and far from the quasi-Lambertian profiles previously reported (Fig. 3), especially for large wedge angles. A good matching can be seen between simulated and experimental values: the patterns are slightly smoother in experimental profiles for allegedly the same reasons already mentioned above (diffraction and polishing defects having been ignored in the simulation). It is interesting to note that the light emitted through the top surface is both predominant over the bottom emission in terms of total power, but also shows angle concentration, *i.e.* the emission cone is narrowing as wedge angle is increased.

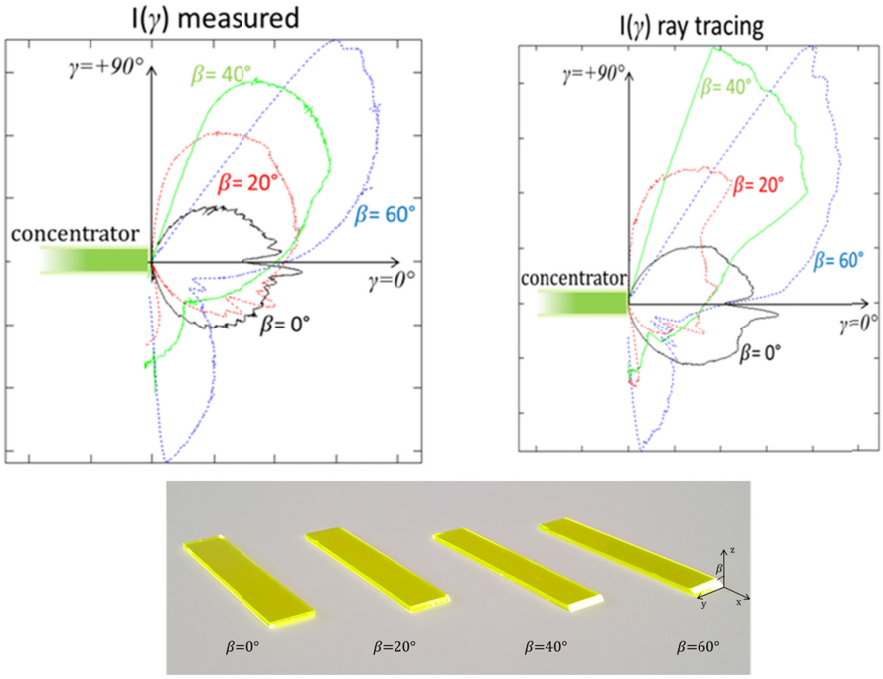


**Fig. 5.** Intensity profiles measured for each wedge angle (left) and calculated using ray tracing simulations (right). These profile sections correspond to one angular coordinate γ about the wedge rotation axis.

The higher intensity is obtained for the wedged sample with β = 60° and an observation angle $\gamma_{max}$ = 52°: it is 2.2 times higher than the average intensity measured around γ = 0° in the reference sample (as the non-wedged LC shows ripples around γ = 0° as discussed earlier, a "Lambertian approximation" was used by taking the average value of intensity around normal incidence). Wedging the LC not only enhances intensity in particular directions but also concentrates the radiation in angle space, which can be a useful feature for some lighting applications. If we define $\Delta\gamma_{FWHM}$ as the angular width at half maximum, it shrinks from 100°

Optics EXPRESS

for the reference down to 52° for the LC with β = 60°. Table 1 summarizes the gain in terms of total extracted power and maximum intensity with respect to the reference unwedged concentrator.

**Table 1. Summary of photometric properties of wedged concentrators compared to the reference polished symmetric slab. $\gamma_{max}$ is the value of $\gamma$ corresponding to the maximum intensity.**

| | β = 0° | β = 0°, frosted edge facet | β = 20° | β = 40° | β = 60° |
|---|---|---|---|---|---|
| ***Gain in extracted power:*** $P_{tot}(\beta)/P_{tot}(\beta = 0)$: from all faces (measured) *$P_{up}(\beta)/P_{up}(\beta = 0)$: from top face only (simulated)* | *1* | *1.5* | *1.5*<br>*1.37* | *1.75*<br>*1.86* | *1.96*<br>*1.78* |
| **Maximum gain in Intensity:** g ($\gamma_{max}$) = I ($\gamma_{max}$) / $I_{ref}$ ($\gamma$~0°) experimentally measured g ($\gamma_{max}$) *simulated* | 1 | 1.5 | 1.2<br>*1.1* | 1.64<br>*1.8* | 2.2<br>*2.2* |
| **Brightness Concentration factor at $\gamma_{max}$ (see text for definition) computed from exp. data** | 5.3 | 8 | 6.5 | 7.1 | 5.9 |

In Table 1 is also reported the 'Brightness concentration factor', calculated as follows. The standard 'concentration factor' C defined as a ratio of irradiances at the output and input area is not an adequate metric when radiation is directional and detected after free-space propagation. It should be replaced by a brightness (or radiance) ratio of output and input radiation fields, or $C_B = B_{out}/B_{in}$. In general, this brightness enhancement factor will depend on the direction of observation, except of course in the case of an angle-independent brightness, that is for a Lambertian source. When both input and output fields are Lambertian, the brightness concentration factor simply equals the classical concentration factor C. It is the case for our reference sample, so that $B_{out,\,ref} = C_{ref}\ x\ B_{in,\,ref}$. The incident brightness for a typical Lambertian source such as LEDs (we write $P_{LED}$ the power of this source) is $B_{in,\,ref} = B_{LED} = P_{LED} / (\pi.S)$ where $S$ is the illuminated surface of the concentrator. For wedged concentrators, $C_B$ will be a more complex function of observation angle:

$$C_B(\gamma) = \frac{B_{out}(\gamma)}{B_{LED}} = C_{ref} \times g(\gamma) \times \frac{\cos\beta}{\cos[\beta - \gamma]} \qquad (3)$$

where $C_{ref}$ is the usual concentration factor for the unaltered symmetric slab, $g(\gamma)$ the gain in intensity at observation angle γ compared to the reference rectangular slab at normal incidence, and the last term a tilting term that takes into account the modification of apparent area. Table 1 reveals that highest brightness is obtained for β = 40° as a compromise between gain in intensity and increase of apparent area. It however remains slightly lower than the brightness achievable with the frosted device of maximal RMS roughness. Hence, depending on the parameter that one wishes to optimize (total extracted power, intensity in a specific direction or brightness), the optimal design will not be the same.

It has also to be noticed that a simple wedge in one direction obviously sharpens the beam in only one direction while keeping the emission pattern in the perpendicular direction coarsely Lambertian. It is illustrated by the simulation of the 3D emission pattern for the 60°-wedged LC reported in Fig. 6.

It is interesting to note that the apparently complex 3D intensity profile is indeed straightforward to interpret when looking back at the angular 3D representation. As soon as the wedge angle is higher than the critical angle, escape cones overlap. Rays that belong to the intersection of two different cones will statistically preferentially exit through the largest surface. Here, the small tilted edge facet and the large top surface respective escape cones have a strong overlap (for α > −3° using notations of Fig. 6 as β = 60° > $\theta_{crit}$ = 33°) whose

Optics EXPRESS

shape is easily recognizable in Fig. 6 (right). A smaller circular-shaped partial erosion at the bottom of the profile corresponds to the intersection with the image of the escape cone of the flat facet opposed to the wedge. It betrays the presence of rays undergoing partial Fresnel reflections on the opposite face and coming back. With this simple example, we can see that the visual representation of rays provided by the representation in k space can help capturing at least qualitatively most of the physics of the light emission of concentrators, before resorting to sometimes very time-consuming numerical ray-tracing simulations.

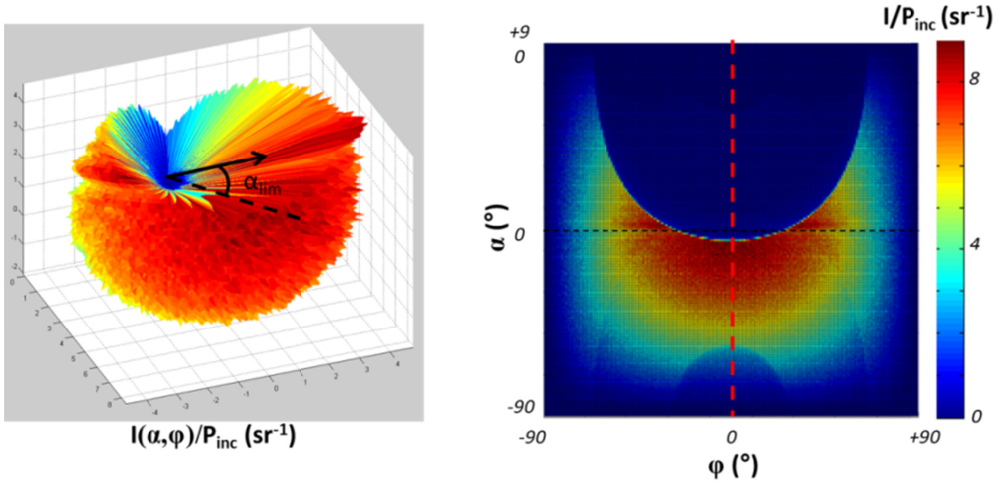


**Fig. 6.** 3D ray diagram of light emitted through the top tilted surface (only) of a Luminescent Concentrator with a wedge angle of 60°. The central direction ( $\alpha = \varphi = 0$ ) corresponds to the normal of the tilted surface, $\alpha$ describes rotation about wedge axis. The circular dark region on top is due to the overlap of the escape cone of the tilted surface with that of the largest top surface.

For further optimization of wedged concentrators while keeping all modifications easily accessible at low cost, wedges in oblique directions (to totally remove trapped rays), or multiple wedges can be considered to optimize the directionality of emission from a Luminescent Concentrator.

## 5. Conclusion

LCs are versatile photonic components that can be used to enhance the brightness available from Lambertian Light sources like arrays of LEDs or OLEDs. Luminescent concentrators can be seen as novel tools in the Light source design toolbox, but this requires the traditional symmetric slab geometry with orthogonal polished facets to be revisited in order to fully take into account the light extraction issue. We investigated the influence of a simple wedge on the output facet, a solution leading at the same time to more power extraction (up to factor of 2 compared to the polished reference) and to a more directional emission (intensity up to x 2.2), in a way that is shown to be very dependent on the wedge angle. Optimum wedge angle ranges between 40° (optimized brightness) to more than 60° (optimized intensity and total extracted power). In comparison, roughening the exit facet allows only a gain in 1.5 in terms of extracted power compared to the reference, but yields the maximum gain in brightness while keeping the source Lambertian.

For the design of Luminescent Concentrators based on low-reabsorption materials, we have presented a simple framework based on an intuitive 3-dimensional representation of rays in angle space that mixes the usual optical indicatrix with the concept of escape cones. It enables making rapid estimates and also conceptualizing different deviations appended to the classical symmetric slab design used in Luminescent solar concentrators. Wedging a

Optics EXPRESS

concentrator appears as a solution that is easily transferrable to any material and that can serve as a source of inspiration for more sophisticated designs of LC-based high-brightness sources.

## Appendix

The ripples observed on Fig. 3 for the reference polished concentrator informs in some way on the "history" of a ray trajectory: for instance, the minimum intensity observed at normal incidence betrays the fact that only rays directly emitted by chromophores without any TIR event can escape the LC with an angle near zero degree. This effect can be very well reproduced with ray tracing simulations (see Fig. 5) and result from the non-uniform distribution of luminescence along the thickness e (1mm) due a strong absorption at 450 nm.

It can be understood easily by drawing the path of rays suffering one or several TIR before escaping the LC. In Fig. 7(a)), we show the rays coming from a single fluorophore (here for simplification in the middle of the LC) and escape without any reflection (grey), with 1 (blue) or two (orange) TIR on the LC large sides. Those rays can also be described as coming from the image points (relatively to the bottom face of the LC in this example) of the initial fluorophore (dotted line). If we expand this representation to multiple reflections on both faces (Fig. 7(b)), we observe in the far field that for some directions the rays having experienced 0, 1, 2 or 3 TIR overlap while for other directions they don't. The result is an inhomogeneous repartition of the energy in any plane parallel to the output facet, materialized by the ripples observed in Fig. 3. The position of maxima depends on source location, hence ripples will be washed out and not seen if the density of luminescence is homogeneous inside the concentrator. It is not the case when absorption is strong: because of Beer-Lambert law, luminescence sources follow an exponential decaying distribution starting at the surface where the excitation light enters the LC (this also explains the large dissymmetry around zero degree). To experimentally check this, we reduced the absorption of the LC by replacing the 450 nm diodes by a Xe discharge lamp followed by a monochromator. It is then possible to excite the LC at 400 nm for example, a wavelength where the Cerium absorption is largely reduced — hence leading to homogenization of the luminescence density along the thickness. We observed in this case (Fig. 8) the disappearance of the ripples for the reference polished, as expected and as also observed with the frosted sample.

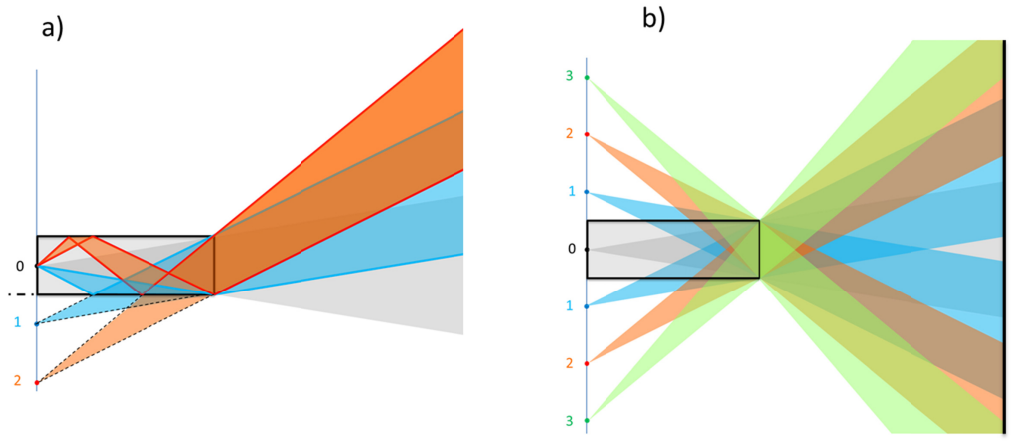


**Fig. 7.** (See text) a) Simple representation of the path of some rays experiencing different numbers of TIR before escaping the LC. In blue, rays suffering only TIR can be represented as coming from the image of the source by the LC large face (point labelled "1"), while rays having bounced twice before exiting can be represented as coming from the point "2" (orange). b) extension of this representation to multiple TIR on both large LC faces.

Optics EXPRESS

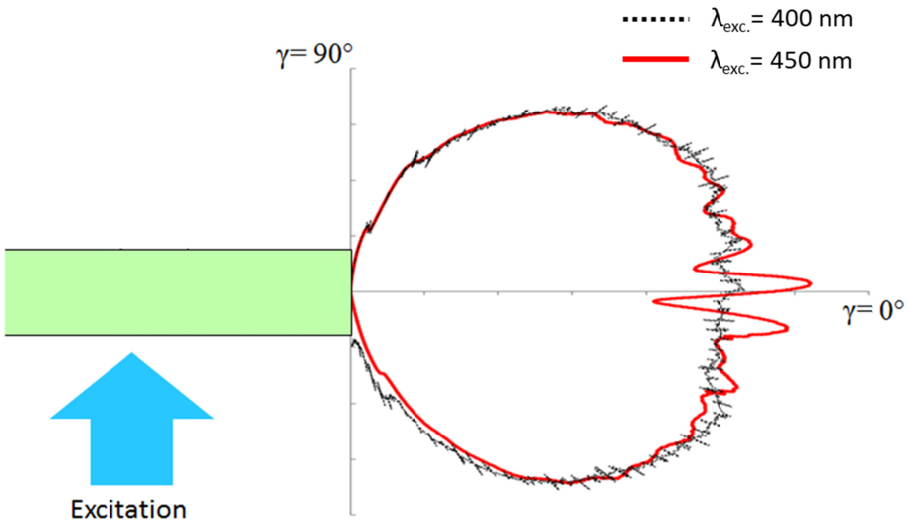


**Fig. 8.** Comparison of the intensity indicatrix under excitation at 450 nm (high absorption coefficient, leading to a localization of the emitting fluorophores mainly near the surface that is illuminated by the source) and at 400 nm (low absorption leading to quasi-homogeneous excitation throughout the LC thickness).

## Funding

Agence Nationale de la Recherche (ANR) (ANR- 2012-BS09-0012-01).

## References

1. J. D. Bullough, "LEDs and automotive lighting applications," *Nitride Semicond. Light. Diodes*, pp. 647–658, Jan. 2018.
2. N. G. Yeh, C.-H. Wu, and T. C. Cheng, "Light-emitting diodes—Their potential in biomedical applications," Renew. Sustain. Energy Rev. **14**(8), 2161–2166 (2010).
3. Y. Yang, G. A. Turnbull, and I. D. W. Samuel, "Hybrid optoelectronics: A polymer laser pumped by a nitride light-emitting diode," Appl. Phys. Lett. **92**(16), 163306 (2008).
4. A. Barbet, A. Paul, T. Gallinelli, F. Balembois, J.-P. Blanchot, S. Forget, S. Chénais, F. Druon, and P. Georges, "Light-emitting diode pumped luminescent concentrators: A new opportunity for low-cost solid-state lasers," Optica **3**(5), 465–468 (2016).
5. P. Pichon, A. Barbet, D. Blengino, P. Legavre, T. Gallinelli, F. Druon, J.-P. Blanchot, F. Balembois, S. Forget, S. Chénais, and P. Georges, "High-radiance light sources with LED-pumped luminescent concentrators applied to pump Nd:YAG passively Q-switched laser," Opt. Laser Technol. **96**, 7–12 (2017).
6. P. A. Haigh, Z. Ghassemlooy, S. Rajbhandari, and I. Papakonstantinou, "Visible light communications using organic light emitting diodes," IEEE Commun. Mag. **51**(8), 148–154 (2013).
7. B. A. Katchman, J. T. Smith, U. Obahiagbon, S. Kesiraju, Y.-K. Lee, B. O'Brien, K. Kaftanoglu, J. Blain Christen, and K. S. Anderson, "Application of flat panel OLED display technology for the point-of-care detection of circulating cancer biomarkers," Sci. Rep. **6**(1), 29057 (2016).
8. J. Chaves, *Introduction to nonimaging optics*. CRC Press, published July 26, 2017, ISBN 9781138747906.
9. J. S. Batchelder, A. H. Zewail, and T. Cole, "Luminescent solar concentrators. 1: Theory of operation and techniques for performance evaluation," Appl. Opt. **18**(18), 3090–3110 (1979).
10. F. Meinardi, A. Colombo, K. A. Velizhanin, R. Simonutti, M. Lorenzon, L. Beverina, R. Viswanatha, V. I. Klimov, and S. Brovelli, "Large-area luminescent solar concentrators based on 'Stokes-shift-engineered' nanocrystals in a mass-polymerized PMMA matrix," Nat. Photonics **8**(5), 392–399 (2014).
11. W. G. J. H. M. van Sark, "Luminescent solar concentrators - A low cost photovoltaics alternative," Renew. Energy **49**, 207–210 (2013).
12. P. Pichon, A. Barbet, J.-P. Blanchot, F. Druon, F. Balembois, and P. Georges, "Light-emitting diodes: a new paradigm for Ti:sapphire pumping," Optica **5**(10), 1236 (2018).
13. E. F. Schubert, *Light-emitting diodes*. Cambridge University, 2006.

Optics EXPRESS


14. K. Saxena, V. K. Jain, and D. S. Mehta, "A review on the light extraction techniques in organic electroluminescent devices," Opt. Mater. **32**(1), 221–233 (2009).
15. X. Chen, B. Liu, Q. Wu, Z. Zhu, J. Zhu, M. Gu, H. Chen, J. Liu, L. Chen, and X. Ouyang, "Enhanced light extraction of plastic scintillator using large-area photonic crystal structures fabricated by hot embossing," Opt. Express **26**(9), 11438–11446 (2018).
16. I. Schnitzer, E. Yablonovitch, C. Caneau, T. J. Gmitter, and A. Scherer, "30% external quantum efficiency from surface textured, thin□film light□emitting diodes," Appl. Phys. Lett. **63**(16), 2174–2176 (1993).
17. S. Möller and S. R. Forrest, "Improved light out-coupling in organic light emitting diodes employing ordered microlens arrays," J. Appl. Phys. **91**(5), 3324–3327 (2002).
18. M. R. Krames, M. Ochiai-Holcomb, G. E. Höfler, C. Carter-Coman, E. I. Chen, I.-H. Tan, P. Grillot, N. F. Gardner, H. C. Chui, J.-W. Huang, S. A. Stockman, F. A. Kish, M. G. Craford, T. S. Tan, C. P. Kocot, M. Hueschen, J. Posselt, B. Loh, G. Sasser, and D. Collins, "High-power truncated-inverted-pyramid (AlxGa1−x)0.5In0.5P/GaP light-emitting diodes exhibiting 50% external quantum efficiency," Appl. Phys. Lett. **75**(16), 2365–2367 (1999).
19. M. Boroditsky, T. F. Krauss, R. Coccioli, R. Vrijen, R. Bhat, and E. Yablonovitch, "Light extraction from optically pumped light-emitting diode by thin-slab photonic crystals," Appl. Phys. Lett. **75**(8), 1036–1038 (1999).
20. D. K. G. de Boer, D. Bruls, and H. Jagt, "High-brightness source based on luminescent concentration," Opt. Express **24**(14), A1069–A1074 (2016).
21. A. Barbet, A. Paul, T. Gallinelli, F. Balembois, J.-P. Blanchot, S. Forget, S. Chénais, F. Druon, and P. Georges, "New scheme for pumping solid-state lasers based on LED-pumped luminescent concentrators," in *Optics InfoBase Conference Papers*, 2014.
22. L. R. Wilson, B. C. Rowan, N. Robertson, O. Moudam, A. C. Jones, and B. S. Richards, "Characterization and reduction of reabsorption losses in luminescent solar concentrators," Appl. Opt. **49**(9), 1651–1661 (2010).
23. T. S. Parel, C. Pistolas, L. Danos, and T. Markvart, "Modelling and experimental analysis of the angular distribution of the emitted light from the edge of luminescent solar concentrators," Opt. Mater. **42**, 532–537 (2015).